OMTM, Volume *29*

Supplemental information

Next-generation poly-L-histidine formulations for miRNA mimic delivery

Vishal Kasina, Aniket Wahane, Chung-Hao Liu, Lin Yang, Mu-Ping Nieh, Frank J. Slack, and Raman Bahal

SAXS MODELS

Scattering intensity, $I(q)$, of a particulate system can be expressed by the multiplication of volumetric concentration, c_{lp}, a contrast factor, $\Delta\rho^2$, form factor $P(q)$ and a structure factor $S(q)$ as

$$I(q) \propto c_{lp} \cdot \Delta\rho^2 \cdot P(q) \cdot S(q)$$

In this study, a core-shell spherical model is chosen for the form factor to analyze the SAXS data of PLGA:PH and PLGA:PH-miR-34a. The best fitting was performed using SasView (https://www.sasview.org/). Due to the low concentration, *S(q)* is set to be unity.

Core-shell spherical model (form factor):

The intensity $I(q)$ for the core-shell spherical is given by:

$$I(q) = \frac{scale}{V} \times F(q)^2 + background,$$

where

$$F(q) = \frac{3}{V_s}\left[V_c(\rho_c - \rho_s)\frac{sin(qR_c) - qR_c\cos(qR_c)}{(qR_c)^3} + V_s(\rho_s - \rho_{solv})\frac{sin(qR_s) - qR_s\cos(qR_s)}{(qR_s)^3}\right],$$

where V_s and V_c are the volume of the whole particle and core, respectively. R_s and R_c are the radius of particles (radius plus thickness) and core radius, respectively. ρ_c, ρ_s, ρ_{solv} are the scattering length density of the core, the shell and the solvent, respectively.

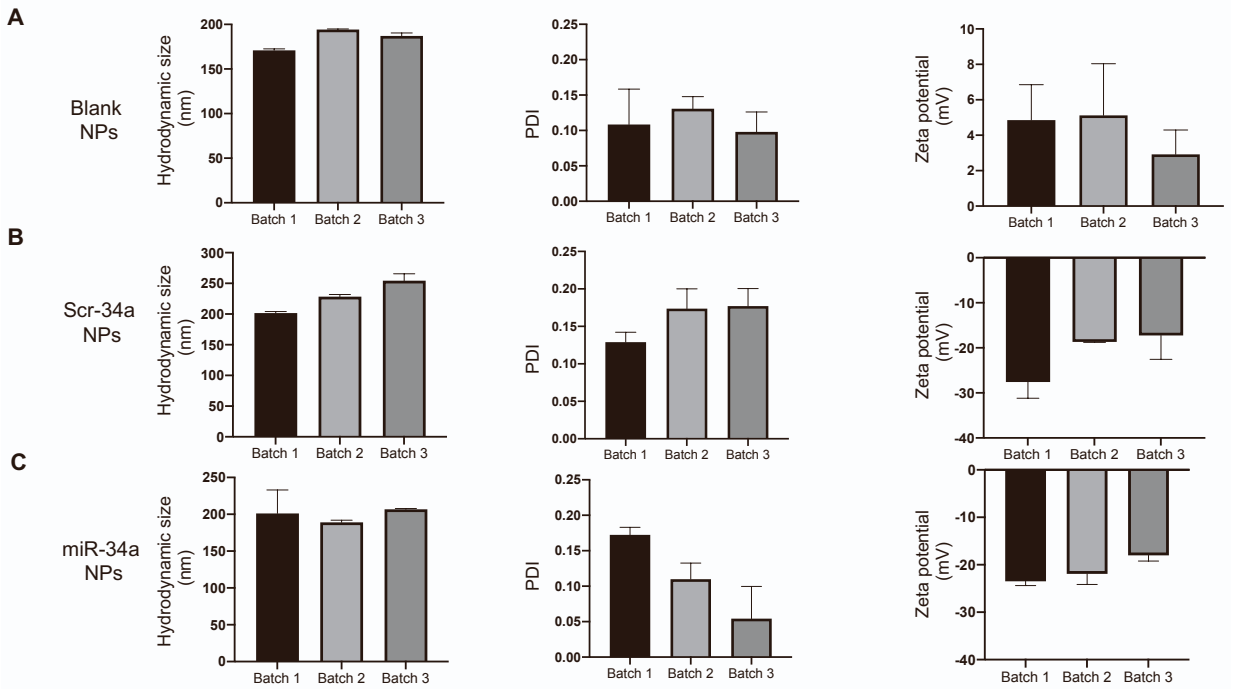

Figure S1. Nanoparticle characterization of different batches. A) Blank NP hydrodynamic size (in nm), polydispersity index (PDI), and surface charge density (in mV). Data is shown as mean ± SD for n=3 samples. **B)** Scr-34a NP hydrodynamic size (in nm), polydispersity index (PDI), and surface charge density (in mV). Data is shown as mean ± SD for n=3 samples. **C)** miR-34a NP hydrodynamic size (in nm), polydispersity index (PDI), and surface charge density (in mV). Data is shown as mean ± SD for n=3 samples.

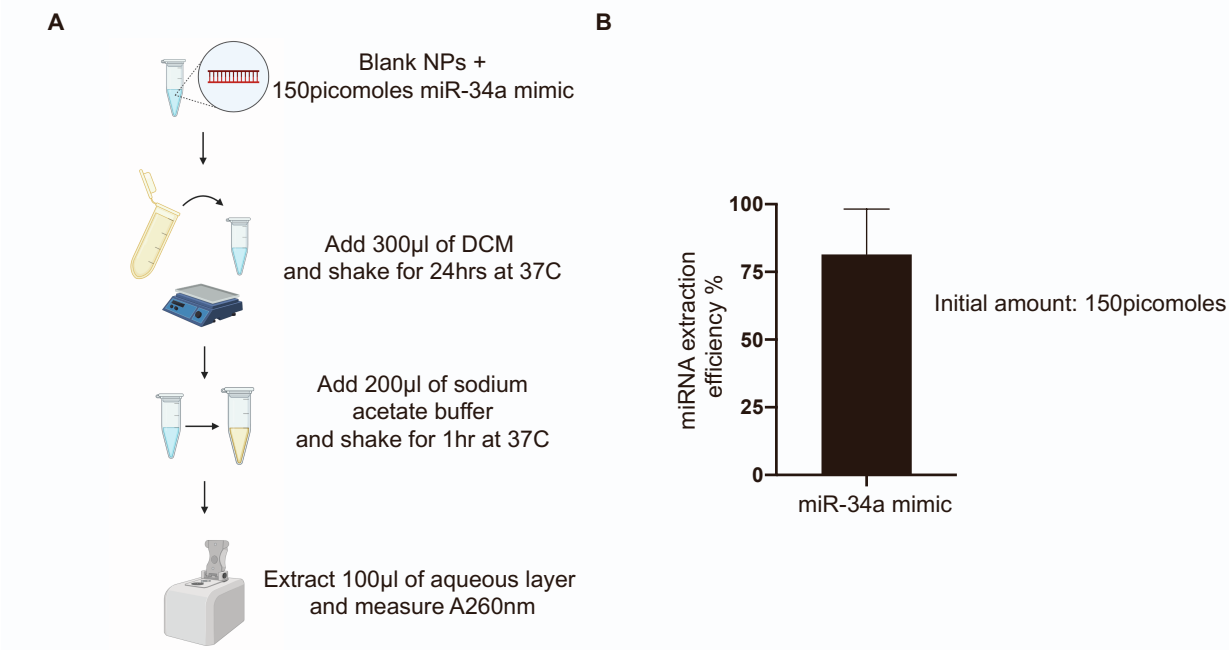

Figure S2: miRNA mimic extraction efficiency. A) Schematic representing the method used to quantify the miRNA mimic in the DCM/sodium acetate buffer mixture. B) miRNA extraction efficiency % when starting with 150 picomoles of miR-34a mimic.

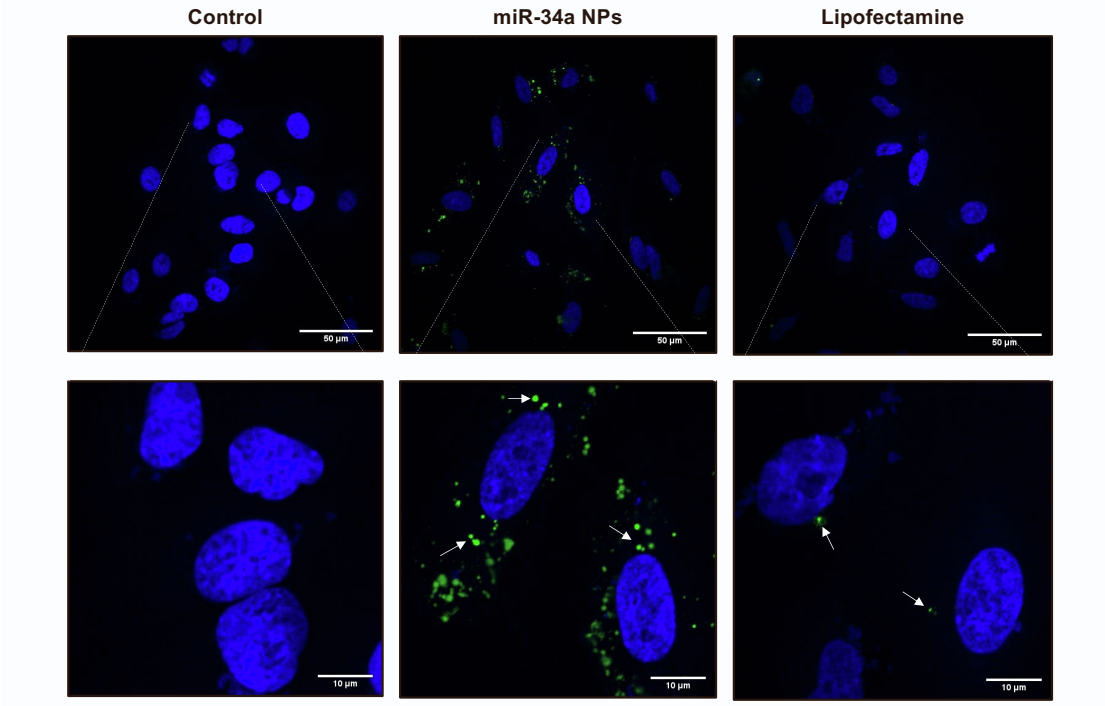

Figure S3. Comparative cellular uptake of miR-34a-FITC in NPs and lipofectamine in A549 cells using confocal microscopy. Cells were treated at an equivalent dose of 300 picomoles of miR-34a-FAM mimic. Green puncta represent miR-34a-FITC undergoing cellular uptake. Blue represents nuclei. The images were taken at 60X and 100X magnification. The scale bar represents 50µm and 10µm for 60X and 100X images respectively.

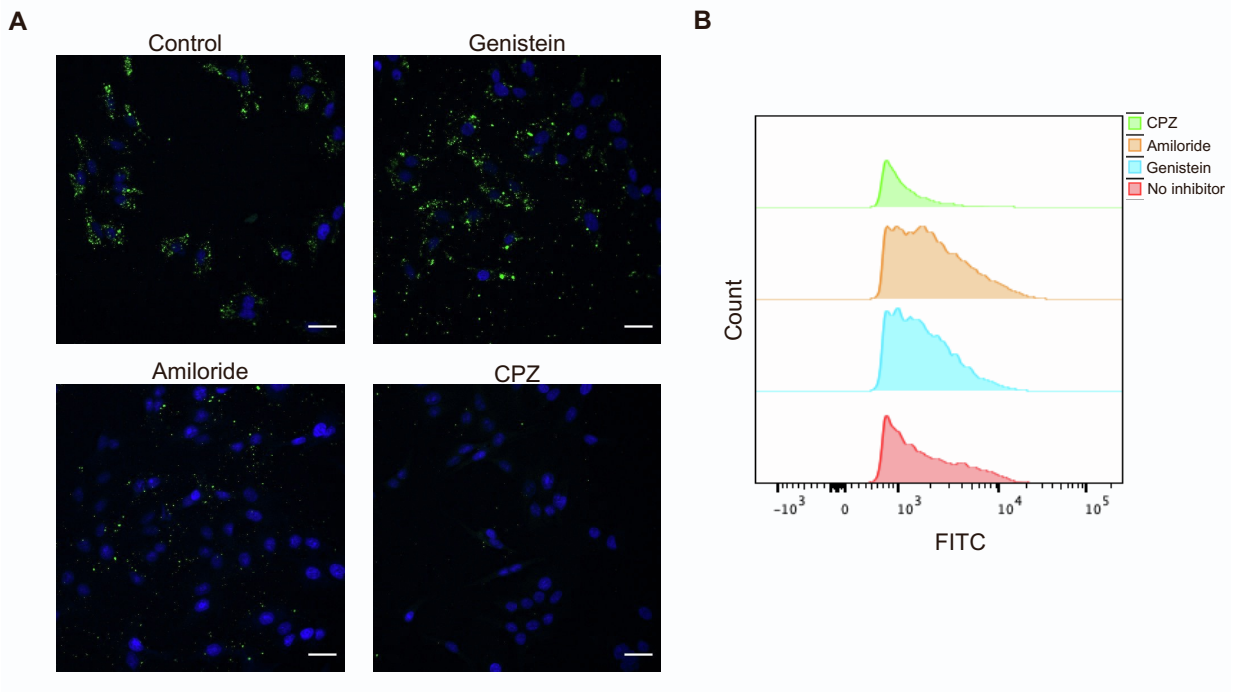

Figure S4: Route of endocytosis of miR-34a NPs A) Endocytosis of miR-34a NPs using confocal microscopy. A549 cells were pre-treated with genistein, amiloride, and chlorpromazine (CPZ) for 30min. a 2mg/mL NP dose of miR-34a-FITC NPs was used. Images were taken at 40X magnification, and the scale bar represents 50μm. Green puncta represent miR-34a-FITC NPs. Blue represents nuclei. B) Endocytosis of miR-34a NPs using flow cytometry. Histogram showing cellular uptake when treated with different endocytosis inhibitors. FlowJo used for quantification of data.

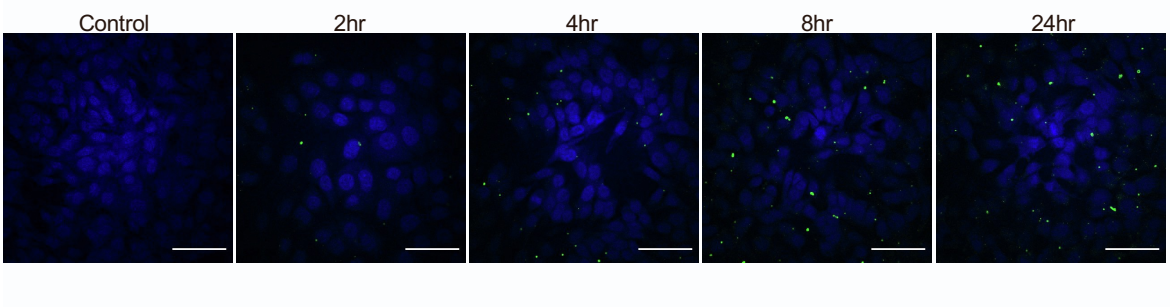

Figure S5. Time-dependent cellular uptake of miR-34a NPs. Cells were treated with miR-34a-FITC NPs for 2hr, 4hr, 6hr, and 24hrs. The scale bar represents 50μm. Green puncta represent miR-34a-FITC NPs. Blue represents nuclei.

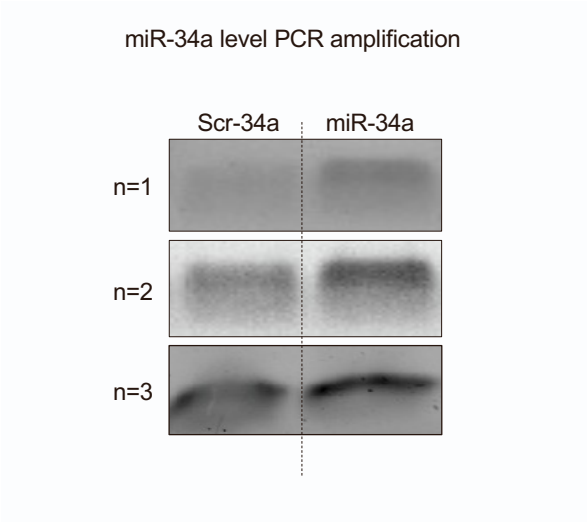

Figure S6. Agarose gel of miR-34a PCR amplification. Blot intensities show the relative miR-34a levels comparing Scr-34a NPs and miR-34a NP treatment. Data is shown for n=3 replicates

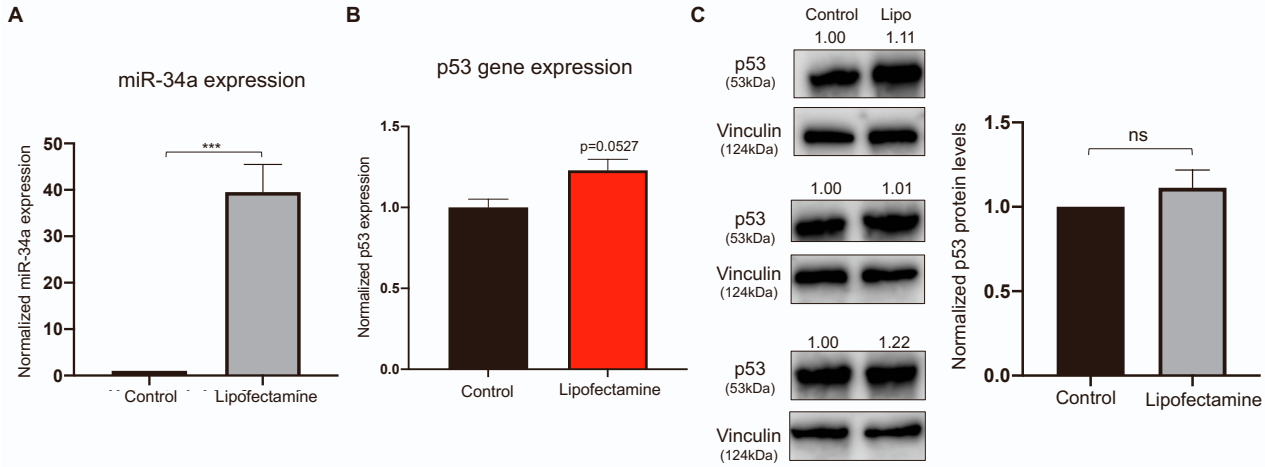

Figure S7. Functional analysis of A549 cells treated with Lipofectamine-transfected miR-34a mimic. A) miR-34a expression using RT-PCR when transfected with miR-34a mimic. Data is shown as mean ± SD. B) p53 gene expression using RT-PCR when transfected with 600 picomoles of miR-34a mimic. Data is shown as mean ± SD. C) p53 protein levels when transfected with miR-34a mimic. Blot intensities are shown above the blot and were quantified using ImageJ software. Unpaired student's t-test was used to determine statistical significance. *, $p<0.05$.

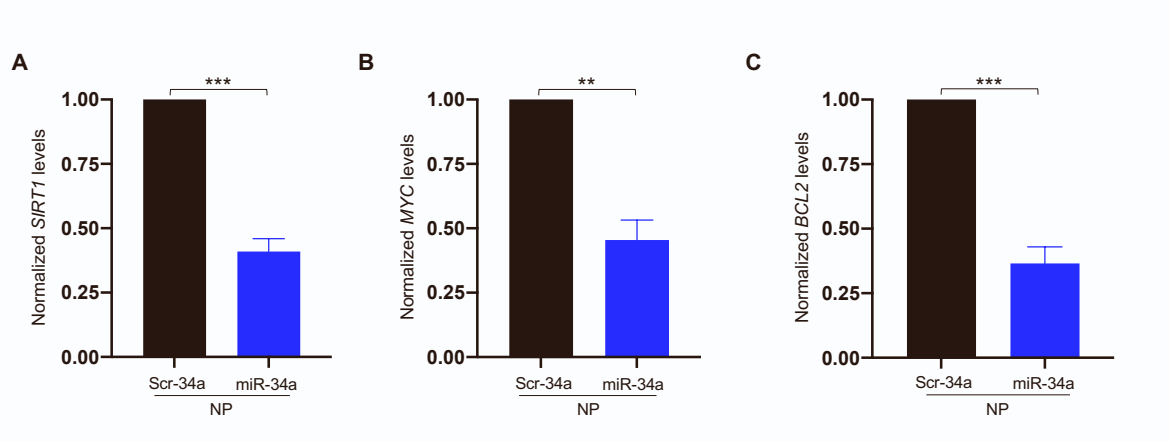

Figure S8. Gene expression of miR-34a direct targets. A) *SIRT1* gene expression in A549 cells after treated with Scr-34a NPs and miR-34a NPs for 24hrs at a 2mg/ml dose. Data is shown as mean ± SD for n=3 samples. **B)** *MYC* gene expression in A549 cells after treated with Scr-34a NPs and miR-34a NPs for 24hrs at a 2mg/ml dose. Data is shown as mean ± SD for n=3 samples. **C)** *BCL2* gene expression in A549 cells after treated with Scr-34a NPs and miR-34a NPs for 24hrs at a 2mg/ml dose. Data is shown as mean ± SD for n=3 samples. Unpaired student's t-test was used to determine statistical significance. **, $p<0.01$; ***, $p<0.001$.

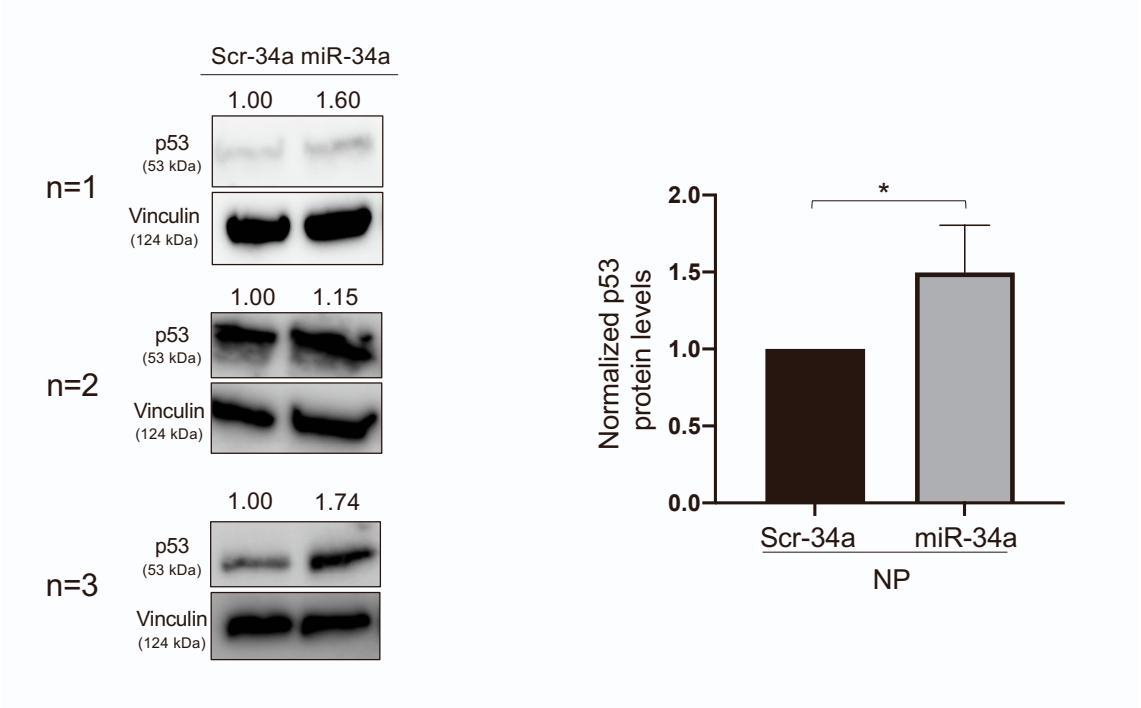

Figure S9. Western blot analysis of p53 protein from A549 cells treated with Scr-34a NPs and miR-34a NPs for 24hrs at a 2mg/mL dose. p53 protein levels are normalized to Vinculin levels. Data represent the mean (n=3) ± SD. Protein blots indicate protein intensity based on pixels per band, quantified using ImageJ. Unpaired student's t-test was used to determine statistical significance. The n=1 blot is shown in Figure 3E. *, $p<0.05$.

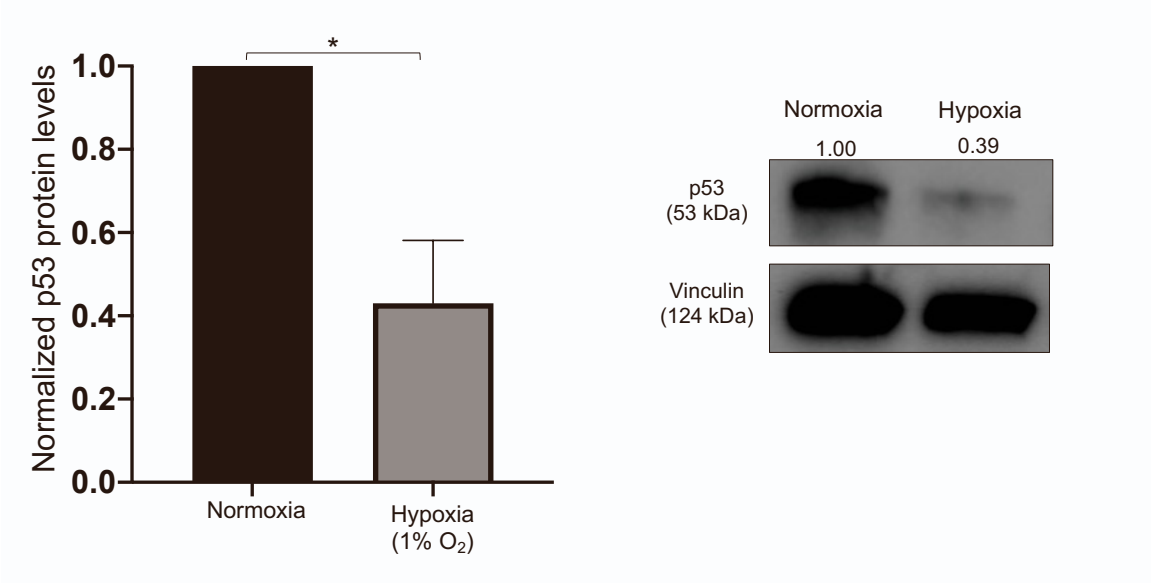

Figure S10. Western blot analysis showing baseline p53 protein levels in hypoxia conditions. Data is represented as mean ± SD (n=3) and normalized to p53 protein levels in Normoxia conditions. Blot intensities were quantified using ImageJ software based on pixels per band. Unpaired student's t-test was used to determine statistical significance. *, $p<0.05$.

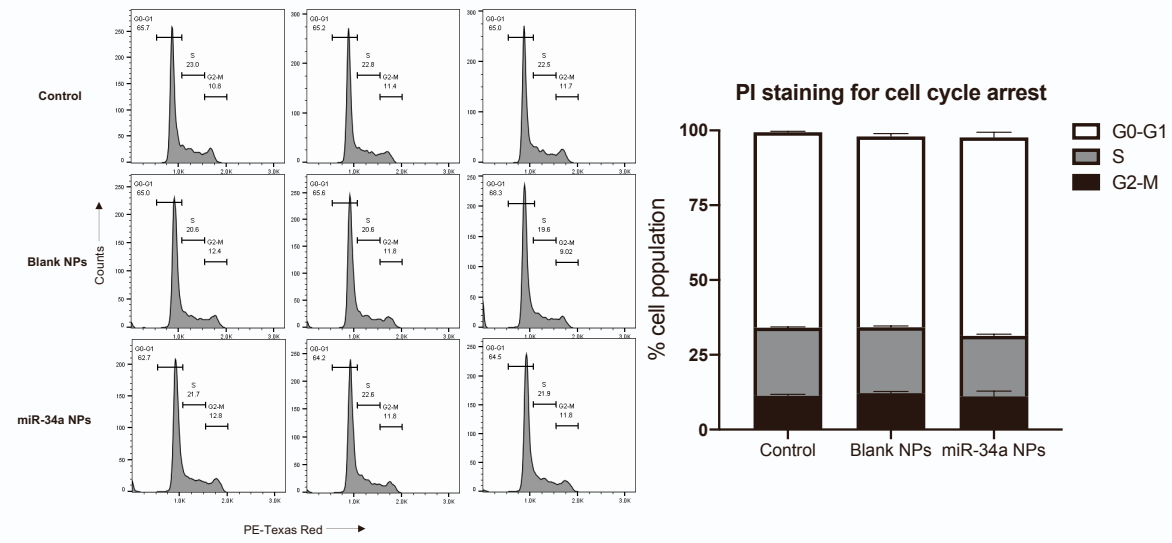

Figure S11. Cell cycle arrest assay using propidium iodide staining. Individual histograms from flow cytometry analysis to quantify cell cycle changes following treatment with miR-34a NPs and BL NPs after 24hrs in A549 cells at a 2mg/mL dose. Cells were stained with propidium iodide and histograms were gated to identify cell populations at different cell cycle phases. Percentage cell populations in G0-G1, S and G2-M phases were plotted. Data represent the mean (n=3) ± SD.

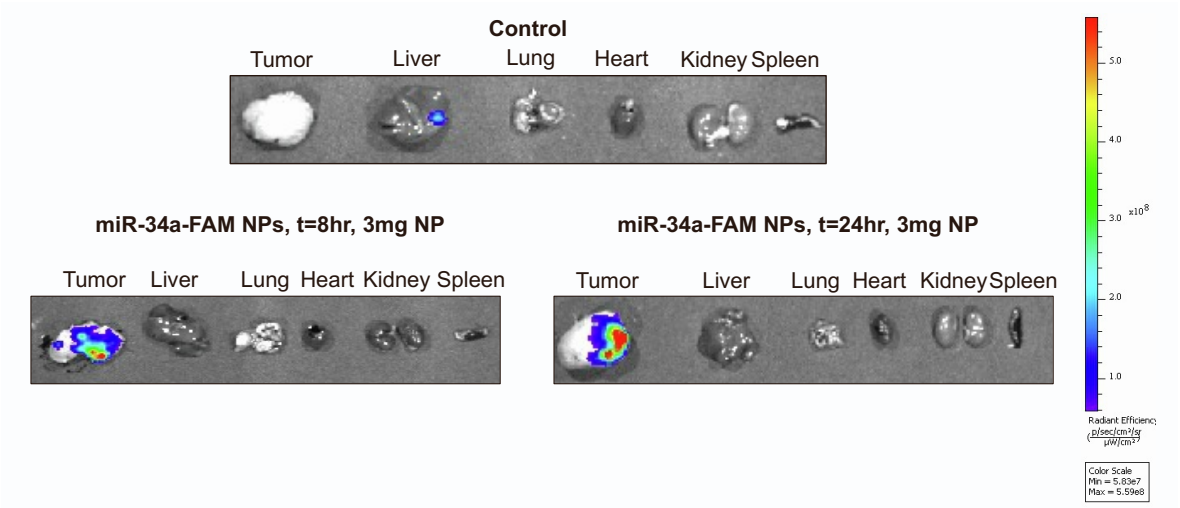

Figure S12: Intratumoral biodistribution of miR-34a-FAM NPs in harvested organs. The images presented are of the tumor, liver, lung, heart, kidney, and spleen and were taken using the Spectrum CT IVIS imager. The mice were treated with miR-34a-FAM NPs at a 3mg NP dose for 8hrs and 24hrs.

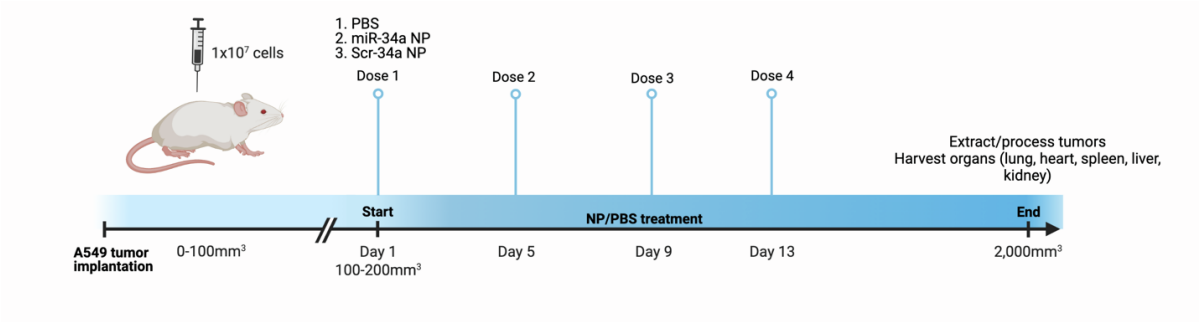

Figure S13. Workflow for *in vivo* efficacy studies in A549 xenograft mice. Mice were treated with PBS, miR-34a NPs, and Scr-34a NPs intratumorally on Day 1, 5, 9, and 13 with 3mg of NPs. Tumor dimensions were recorded daily to measure volume. After the tumors reached 2,000mm^3, the tumors were processed and the lungs, heart, spleen, liver, and kidney were harvested.

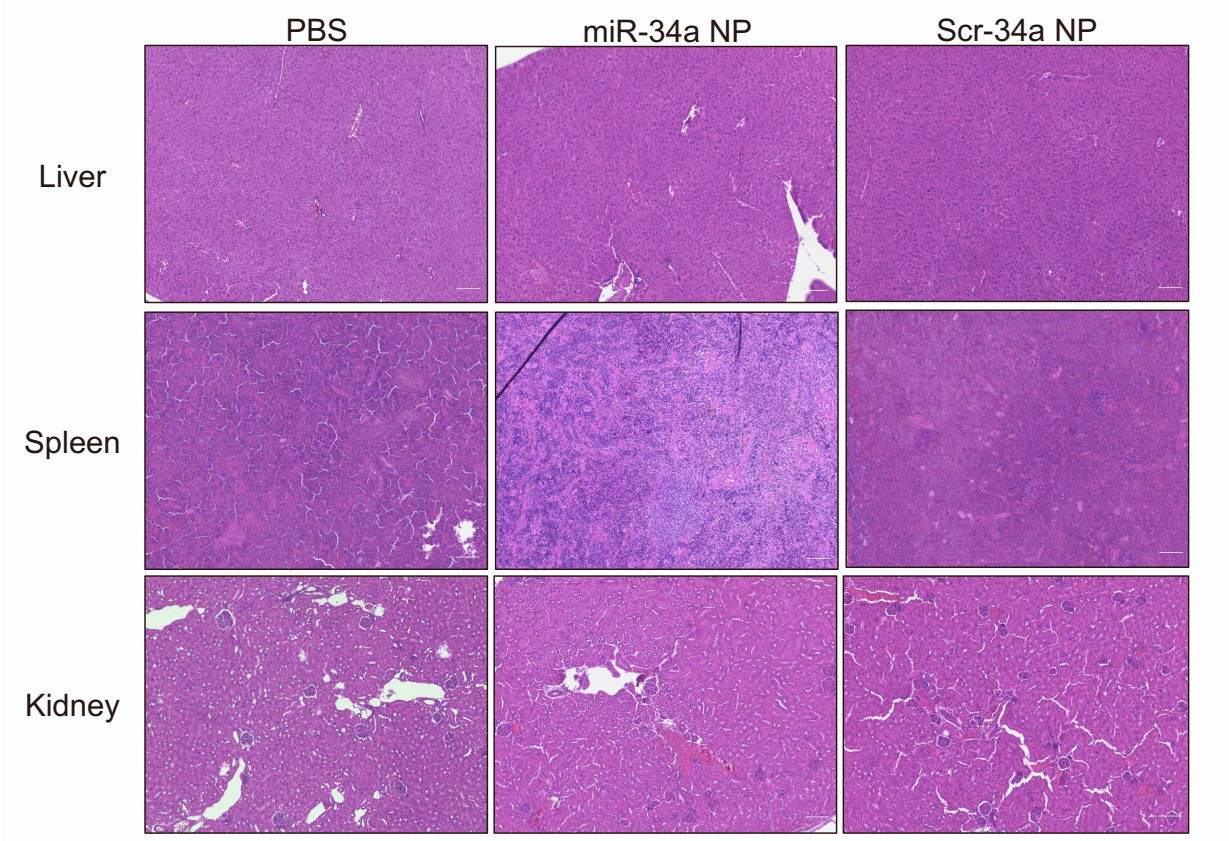

Figure S14. H&E staining of liver, kidney and spleen after intratumoral administration of PBS, miR-34a NP, and Scr-34a NP. A 3mg NP dose was injected intratumorally. Images were taken at 10X magnification. The scale bar represents 100μm.